Robotics and Computer–Integrated Manufacturing 93 (2025) 102899

Contents lists available at ScienceDirect

Robotics and Computer-Integrated Manufacturing

journal homepage: www.elsevier.com/locate/rcim

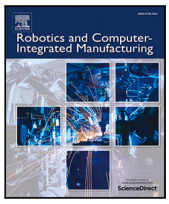

Automating the hand layup process: On the removal of protective films with collaborative robots

Renat Kermenov [a], Sergi Foix [b], Júlia Borràs [b], Vincenzo Castorani [c], Sauro Longhi [a], Andrea Bonci [a,*]

[a] Università Politecnica delle Marche, Via Brecce Bianche 12, Ancona, 60131, Italy
[b] Institut de Robòtica i Informàtica Industrial, C/ Llorens i Artigas 4-6, Barcelona, 08028, Spain
[c] HP Composites S.p.A., Via del Lampo, Z.Ind.le Campolungo, Ascoli Piceno, 63100, Italy

ARTICLE INFO

Keywords:
Composite manufacturing automation
Collaborative robotics
Hand layup process
Protective film removal
Composite manufacturing

ABSTRACT

This paper explores the issue of protective film removal in the hand layup process for composite parts production. The hand layup process, involving the assembly of prepreg plies onto a mold, is a skill-intensive task performed by multiple expert workers. A significant limitation of this method is its low repeatability, which impacts both the consistency and quality of the final product. The current research trend has the objective of developing autonomous or semi-autonomous layup cells to enhance process consistency, reduce production costs, and improve product quality.

Despite all this interest in bringing automation in composite manufacturing, an area left relatively unexplored is the removal of protective films from prepregs. The plies used in the hand layup process, are generally covered by those films that are removed by the workers during the manual layup activity. The manual removal of protective films from prepregs is a tedious and valueless task, which represents a bottleneck in achieving full or semi-automation of the layup process. For this reason, an autonomous or semi-autonomous cell needs to perform it to be market-relevant.

In this work, we propose a new effective method for initiating the peeling and integrate this method into a complete framework for the removal of protective films. This solution is designed to be easily integrated into a variety of existing cells. Finally, we validate our framework with an experimental proof of concept (PoC) which makes use of two collaborative robots for task execution.

1. Introduction

Bringing automation into the lamination process of composite manufacturing is a crucial step to improving quality standards and driving down production costs. The current automation technologies employed by companies are primarily confined to automated tape layup (ATP) and automated fiber placement (AFP) [1]. However, these solutions require substantial financial investments and have inherent technological constraints. The former can make it challenging to achieve a return on investment, especially in low-volume production scenarios. The latter's limitation consists of its suitability which is primarily confined to components with simple geometries, such as flat or single-curved shapes.

Subsequently, a significant segment of composite parts production still leans heavily on the "hand layup" (Appendix A) [2] of pre-cut prepregs (Appendix A). This approach involves highly specialized human workers but faces challenges to consistently meet quality standards due to the variability inherent in the process. Studies by Elkinton et al. [2] emphasize the profound impact of human factors on this process, while de Kruijk [3] has underscored the need for automation to enhance both the process repeatability and quality assurance. Economically, the adoption of automation promises substantial cost savings. Cambell [4] has highlighted that hand layup typically accounts for 40–60% of the fabrication cost, depending on the size and complexity of the part. The potential savings, even with just partial automation, are thus significant. It is not surprising that automated strategies have captured researchers' focus over the past three decades.

In 2017, Elkinton et al. [5] published a comprehensive survey, revealing that many promising solutions have been identified, but none of these seems ready for the market. The prevalent issue is their applicability, which often is restricted to specific shapes, making them less versatile compared to manual layup. More recently, with strides in robotics, perception, and new paradigms aligning with Industry 4.0 or

* Corresponding author.
E-mail address: a.bonci@univpm.it (A. Bonci).
[1] https://www.drapebot.eu/

https://doi.org/10.1016/j.rcim.2024.102899
Received 10 February 2024; Received in revised form 8 August 2024; Accepted 4 November 2024
Available online 4 December 2024

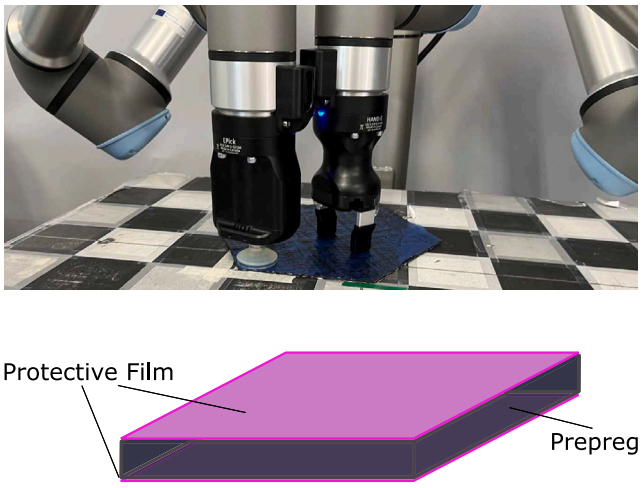

Fig. 1. Top: Our robot framework while performing the task. Bottom: Representation of the ply covered by protective film in both faces.

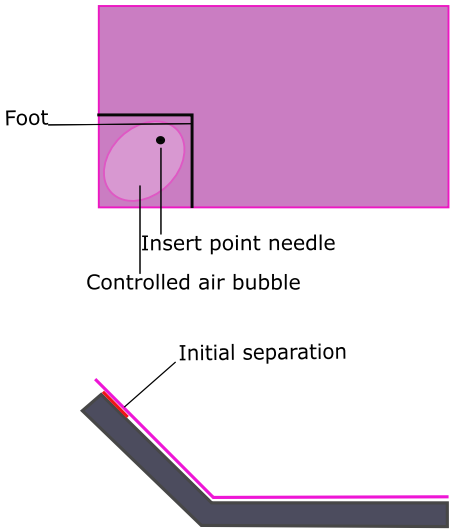

Fig. 2. Two distinct methods for starting the removal of the backing paper: the top image illustrates the approach using air bubbles produced by a needle, while the bottom image utilizes mechanical bending.

5.0, novel approaches have emerged. Malhan et al. [6,7] proposed a multi-robot cell for automating the hand layup process. "DrapeBot"[1] is a European Project started in 2021, that aims at human–robot collaborative draping in the context of carbon fiber production. Such collaborative settings seem promising: robots can assist humans in transporting larger plies enhancing placement accuracy and reducing the labor cost. Several works have been developed in such a direction. De Schepper et al. [8] implemented a control system that considers the human pose and the wrench, while Nicola et al. [9,10] estimate the fabric state using the depth image. Markis et al. [11] and Ansronas et al. [12] use a model-based approach, estimating the ply pose with a mass–spring-dumper model. Papadopoulos et al. [13] developed a complex end-effector for human–robot ply co-transportation and layup. Additionally, the emerging Point Cloud technology offers exciting prospects for real-time process monitoring and quality control in autonomous or semi-autonomous layup cells [14,15].

However, an area left relatively unexplored is the removal of protective films from prepregs. Indeed, the prepregs are generally protected by thin films, as shown in Fig. 1, which are generally removed in situ during the hand layup. These films are typically made of polyethylene (a prevalent plastic type) or paper. Buckingham and Newell [16] initially pinpointed the complexity of the backing paper removal in 1996, emphasizing the intrinsic challenges faced when initiating the peeling process in industrial settings. In 2013 Bjornsson et al. [17] found an effective way to initialize the peeling of backing papers by exploiting the mechanical bending of the ply and then continuing the task with the assistance of a vacuum table. However, this approach is heavily tied to the fully automated cell outlined in the same study. As such, it presents challenges when attempting to integrate it into manufacturing environments where manual labor still plays a significant role. In the same year, Ward et al. [18] conducted an empirical investigation into the techniques workers deploy to detach the protective films during the manual layup process. Drawing inspiration from their observations, they formulated a conceptual approach for automating the procedure. This method integrates the use of cold air, a suction cup, and a sharp tool. In the survey of Elkinton [5] this task is still considered a challenge, despite notable solutions have been found.

The objective of this study is to advance the topic of protective film removal, focusing on plastic films, with an emphasis on versatility and cost-efficiency. Here are the main contributions of this work:

1. Development of a comprehensive framework for the removal of plastic films, outlined in Section 4, with an innovative approach to initiate the peeling process.
2. Provide an experimental PoC for this framework, conducting a series of 40 tests with two collaborative robots to assess the accuracy of the proposed method.
3. Present a series of observations that are both theoretically derived from the peeling equation (that will be introduced in Section 3.3) and experimentally validated, providing valuable insights for further research activities in addressing this issue.

The remainder of the paper is organized as follows: Section 2 offers a detailed review of existing solutions found in the research literature, along with some technical details. Section 3 defines the problem of film removal, examining it from both a practical perspective in an industrial environment and from a theoretical standpoint through the exploration of the peeling equation. Section 4 presents our conceptual solution to the problem. Detailed experimental aspects are covered in Section 5, which includes the experimental setup, the pseudocode of the algorithm utilized (derived from the concepts in Section 4), and an analysis of the experimental outcomes. Lastly, Section 6 concludes the paper.

2. Related works

In 1996, Buckingham et al. [16] introduced an automated system for composite parts production, which had the added feature of backing paper removal. They segmented this task into two primary stages: peeling initiation and peeling continuation. The initiation stage was pinpointed as the more challenging of the two. Later, in 2013, Björnsson et al. [17] proposed two methods for peeling initiation tailored for their automated setup. The first method utilized air injection through a needle, creating an air bubble that effectively separated the two layers, as depicted on the upper side of Fig. 2. A mechanical foot was employed to safeguard the fibers and direct the airflow effectively. The second approach relies on mechanically bending the materials, causing a slight separation between the backing paper and the prepreg, as illustrated on the lower side of Fig. 2. Following this initial separation, the peeling continuation was achieved using a combination of a vacuum gripper and a clamp. However, while effective for removing the backing paper, this method is not entirely suitable for plastic films. Predominantly used in woven prepregs, these protective films are noticeably thinner and more flexible than backing paper. Our manual experiments confirmed that mechanical bending is ineffective for initiating the peeling of these films. This technique relies on the fact that the backing paper has a non-negligible thickness and stiffness, which makes them (prepreg and

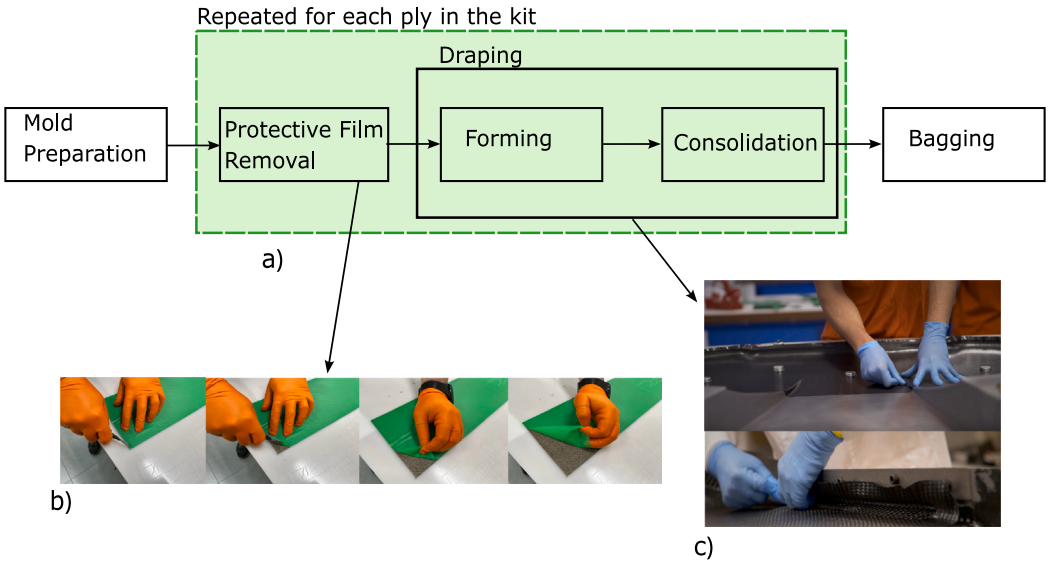

Fig. 3. Lamination department workflow.

baking paper) slide on each other after the deformation. On the other hand, due to its high flexibility and thinness, the plastic film sticks to the prepreg even after being bent. Furthermore, as Kupzik et al. [19] also found, the vacuum gripper was not efficient in the continuation of the peeling process. The film's low bending resistance led to its deformation when a suction cup attempted to grasp it, causing a loss of the vacuum.

Again, in 2013, Ward et al. [18] conducted an empirical investigation into the techniques used by the workers to separate the protective film during the manual layup process. Their research focused on the insights and skills laminators acquired over time. Their proposed solution combined cold air, a suction cup, and a blade. The cold air played a crucial role in reducing the tackiness of the prepreg but also making the film stiffer. Cooling the film decreased its elasticity, facilitating the vacuum gripper's task. Concurrently, the drop in temperature reduced the prepreg's tackiness. Then, the initial separation was aided by the vacuum gripper and furthered by inserting a blade between the prepreg and film.

Kupzik et al. [19] tried different solutions for plastic film removal, termed "backing foil" in their study. They tested many techniques in their research and concluded with the identification of rotating brushes as a promising tool for peeling initiation, combined with a custom clamping gripper for continuation.

A similar issue is present in Flexible Printed Circuit Board (FPCB) assembly, which demands the automated removal of protective films. Both scenarios deal with detaching a film from a flexible substrate. The employment of rotating sanding methods [20,21] in this domain could potentially offer valuable insights for our current challenge.

3. Problem statement

This section provides an in-depth contextual analysis of the issue. We begin with an overview of the lamination process of composite manufacturing, using the "HP Composite S.P.A". production line as a case study. HP Composites is an Italian medium–large company that produces composite components primarily for the automotive and motorsport markets. Following this, we delve into the specific challenges associated with the removal of plastic film from prepregs, ensuring the reader grasps the challenges and origins of these complications.

3.1. Lamination phase

Plies are precisely cut from a prepreg roll using automated machinery and are then grouped into kits, either manually by a human operator or through automated equipment. Once assembled, these kits are forwarded to the lamination department. There, expert workers laminate the plies into the mold. When we talk about automation attempts, this procedure is typically divided into two stages. The term 'draping' encapsulates both of the following stages:

- *Forming*: Here, the ply is retrieved from the kitting table and integrated into the mold. This is not a simple placement. The ply is simultaneously positioned and molded to align with the mold's geometry, which usually has a three-dimensional shape. The complexity of the mold's shape directly affects the complexity of this task.
- *Consolidation*: In this phase, the ply is securely affixed either to the mold or an already placed ply. The worker applies local pressure to conform the ply to the mold, in particular in high curvature positions and ensures that all possible trapped air under the ply's surface is eradicated. This pressure can be applied either with the worker's hand or with a specific tool [22].

Diving deeper into the traditional lamination process, as schematically represented in Fig. 3-a, it becomes evident that draping is part of a more complex procedure. Initially, the mold surface is visually inspected to ensure that is perfectly clean, followed by the application of an anti-adhesive agent to prevent resin adherence (Mold Preparation phase). Subsequently, the laminators start the hand layup task which involves removing the protective film (as shown in Fig. 3-b) and performing the draping (illustrated in Fig. 3-c). In this manual process, this film is typically removed right during the draping activity. This step, seemingly a routine, is incredibly complex to automate. However, we observed that numerous modern and emerging automated solutions have overlooked this procedure. Understanding this step well is crucial to the real-world application and making the solutions market-relevant. Finally, when the laminate is finished, it is enclosed in a vacuum bag and sent to the curing process (Appendix A).

3.2. Protective film removal

All plies delivered to a lamination department are covered with protective films on both sides, as depicted in Fig. 1. The ease of film

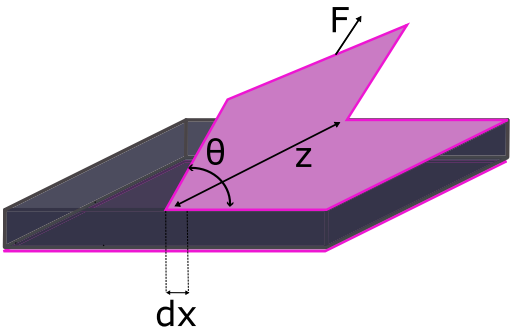

Fig. 4. Rectangular ply covered by protective film in both faces.

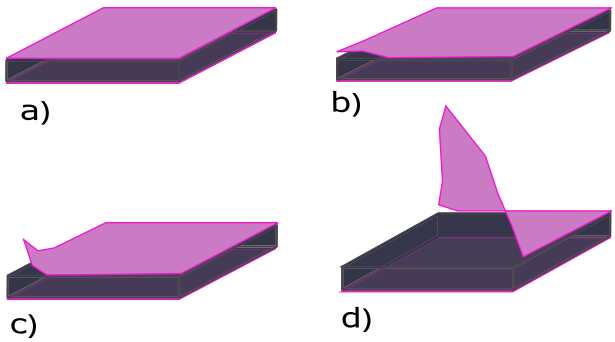

Fig. 5. All the phases of the proposed solution for film removal. (a) Initial state (b) Peeling initiation (c) Elevation of the corner (d) Peeling continuation.

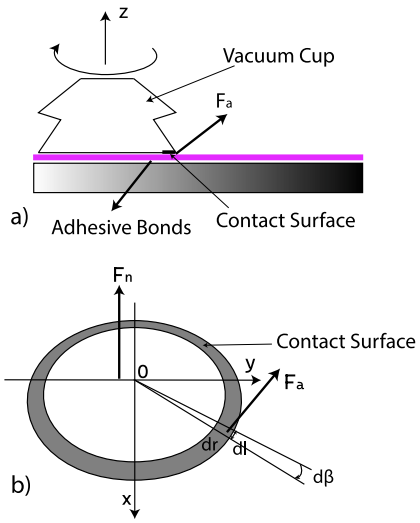

Fig. 6. (a) Suction cup while rotating around z-axes. (b) In gray the contact surface between the suction cup and the protective film. During the rotation, a friction force F_a is generated in the opposite direction. The friction depends on the normal force F_n.

removal is affected by various factors, including prepreg stiffness, ply shape and size, and film type. The primary challenge in this process is the tackiness of the prepreg [18], which is significantly influenced by environmental conditions. For instance, the tackiness of the prepreg is highly sensitive to temperature due to the viscoelastic nature of the polymer [23]. The manual film removal process can be divided in two stages: initiation and continuation. The initiation phase is particularly challenging, requiring the operator to use all their tactile and visual skills for successful removal. Additionally, tools like cutters and ice spray are often employed to facilitate the task. Fig. 3-b depicts the typical sequence of steps involved in the manual process.

3.3. Peeling equation

Consider a scenario where a thin elastic film is being peeled away from a substrate. The peeling occurs at an angle θ under a constant force F, as depicted in Fig. 4. Let us analyze the energy implications when a section $\mathrm{d}x$ is peeled away:

$$W_F = F(1+\cos\theta)\mathrm{d}x + F(1+\cos\theta)\mathrm{d}x_{def} \tag{1}$$

describes the work W_F executed by the force during this peeling action and $\mathrm{d}x_{def}$ represents the deformation of the film. On the other hand, the equation:

$$W_S = -zR\mathrm{d}x \tag{2}$$

denotes the energy W_S of the adhesive surface.

Here, z is the film's width, and R stands for the energy release rate, which tends to rise as the peeling speed $\dot{x}$ increases [24,25]. By applying energy conservation, we can derive the following relationship between the applied force and the geometrical and kinematic quantities involved in the peeling process:

$$F(1+\cos\theta)\mathrm{d}x + F(1+\cos\theta)\mathrm{d}x_{def} - zR(\dot{x})\mathrm{d}x = 0. \tag{3}$$

In this equation, the term $\mathrm{d}x_{def}$ depends on the material properties, F and $R(\dot{x})$. However, considering that plastic films are generally inextensible or little extensible, we can neglect the elastic term [25] since $\mathrm{d}x_{def} \ll \mathrm{d}x$. The Eq. (3) becomes:

$$F(1+\cos\theta) - zR(\dot{x}) = 0. \tag{4}$$

4. Proposed solution

The solution here proposed is based on the ability to merge with the current production framework effortlessly. Typically, laminators are responsible for on-the-spot removal of the protective film, executed right before the ply is draped over the mold. In line with this, our strategy is fashioned around tools that are already used in automating the manual layup process. As stated in [26] the vacuum grippers are the most used. Their key advantage lies in the capacity to grasp an object from just one side, which becomes essential when dealing with flat entities where usually only one side is available. Additionally, their cost-effectiveness adds to their widespread adoption. While very effective in picking up the ply, they are not the best choice when it comes to forming the ply into the mold. During this stage, tension should be applied to the ply to make it adhere to a 3D mold. The vacuum gripper fails to offer a firm grip, resulting in the object sliding upon the application of lateral forces.

With this premise, we decided to use a combination of a two-finger gripper and a vacuum gripper. We have divided the problem into the following four distinct phases:

1. **Step one:** *Peeling initiation*: This initial phase aims to break the adhesive bond between the protective film and the prepreg at one corner, setting the stage for subsequent elevation. The successful completion of this step can be visualized in Fig. 5-b.
2. **Step two:** *Elevation of the corner*: Once one corner of the prepreg is been initiated with success, the next objective is to raise the corner of the film, as represented in Fig. 5-c.
3. **Step three:** *Grasping*: The raised corner from the previous stage is firmly grasped by the two-finger gripper.
4. **Step four:** *Peeling continuation*: Finally the film is separated from the prepreg as shown in Fig. 5-d.

In the following Subsections, we provide details about each step.

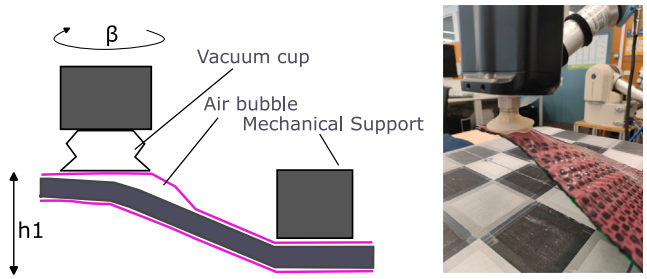

Fig. 7. Step one of the proposed solution: Air bubble formation through mechanical bending with the vacuum gripper.

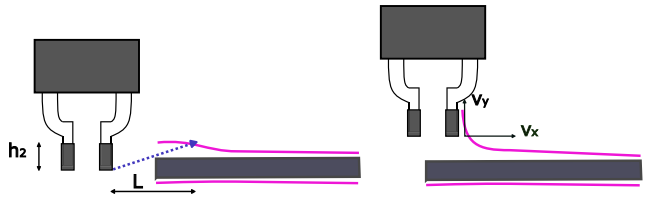

Fig. 8. Step two of the proposed solution: The elevation of the corner is achieved through the impact between the gripper and the plastic film. The left figure represents the starting position of the gripper with respect to the ply corner. The right figure shows the ideal final impact and their velocity components of the gripper during elevation trajectory.

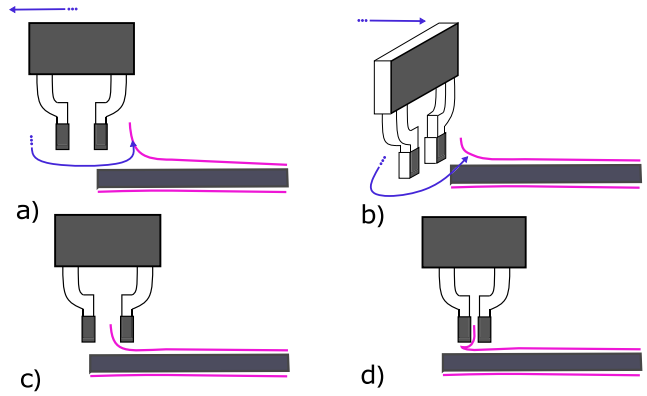

Fig. 9. Step three of the proposed solution: Once the corner is up, the two-finger gripper has to maintain the corner and, at the same time reach the grasping position. Drawings (a) (b) represent the gripper spinning around its Z axis, while (c) and (d) represent the grasping action.

4.1. Step one: Peeling initiation

To start the peeling process, our starting point is a corner. This choice is frequently observed in literature [16–18] and also among the manual workers. This choice can be justified by rearranging Eq. (4) as follows:

$$F = \frac{zR(\dot{x})}{(1+\cos\theta)}. \tag{5}$$

As we move closer to the corner, the width z decreases, hence, from Eq. (5), this results in a decrease of the force F needed to crack the adhesive bond, simplifying the initiation of peeling.

At this stage, the film's corner is not yet available for grasping. Manual workers often rely on friction to detach the corner. To optimize the initiation, we used the friction generated by a vacuum cup. Mantriota et al. [27] provide a detailed friction model for a circular vacuum cup. We will introduce additional assumptions specific to our scenario to simplify the model and relate it to the adhesive bonds between the film and the ply. Consider a suction cup rotating around its z-axis while holding the corner surface of the film, as illustrated in Fig. 6-a. The friction force F_a between the cup surface and the film acts in the opposite direction with respect to the rotation direction. The work executed by the friction during the rotation is given by:

$$W_{F_a} = M_{Fa}\mathrm{d}\beta. \tag{6}$$

where M_{F_a} is the torque related to the friction and $\mathrm{d}\beta$ is the rotation angle. By applying Newton's second law for rotation, $M_{F_a} = I\alpha$, where α and I are angular acceleration and the inertial moment respectively, we get:

$$W_{Fa} = I\alpha\mathrm{d}\beta. \tag{7}$$

Considering the energy released during the detachment,

$$W_S = -R(v)\mathrm{d}A, \tag{8}$$

where dA is the area detached during the motion and v velocity of detachment (denoted as $\dot{x}$ in Eq. (4)), and assuming negligible the film deformation, we can apply the energy conservation law:

$$I\alpha\mathrm{d}\beta = R(v)\mathrm{d}A. \tag{9}$$

From this, we can observe that increasing the angular acceleration α results in augmenting the film area detached $\mathrm{d}A$ from the prepreg, which is our final objective. However, this model works until the suction cup surface does not slip on the film surface. The friction torque is related to the friction force, $M_{Fa} = F_a r_G$ (the rotation axis is orthogonal to the friction force), where r_G is the radius of the suction cup and the friction force non-slipping condition follows the relation:

$$F_a \leq \mu F_n \tag{10}$$

where μ is the friction coefficient and F_n is the normal force between the suction cup and the film surface, as represented in Fig. 6-b. Because F_n depends on the pressure p generated by the suction cup, and, assuming it is uniform across the circular surface, we have $F_n = \pi r_G^2 p$. In case of incipient slipping of the suction cup (assuming that we are operating at maximum angular acceleration α before slipping), the relation (10) is verified with the sign of equality:

$$F_a = \mu F_n = \mu\pi r_G^2 p. \tag{11}$$

Writing the friction work as $W_{Fa} = F_a\mathrm{d}l = F_a r_G\mathrm{d}\beta$, and replacing it in the energy conservation low, we have:

$$\mu\pi r_G^3 p\mathrm{d}\beta = R(v)\mathrm{d}A. \tag{12}$$

The Eq. (12) shows as the increase of the friction coefficient μ and the vacuum level p bring to higher $\mathrm{d}A$. Increasing the radius r_G would deserve more attention and analysis because it would affect the vacuum level p if the vacuum flow is maintained the same.

Further, we capitalized on a phenomenon we observed: when the ply is lifted and bent, as depicted in Fig. 7, an air bubble forms. In the presence of air bubbles, the protective film and the prepreg are not in contact and the adhesive bond is locally broken. To optimize the rotational movement, the end effector performs a vertical linear movement at the same time. while the other arm acts as mechanical support to hold the prepreg against the table. This action detaches the film at the corner and is characterized by two movement parameters of the vacuum gripper: β, which represents the angular rotation, and h_1, which measures the distance of the vertical linear movement.

4.2. Step two: elevating the corner

After detaching the film's corner, our next objective is to elevate it for a secure grasp. To achieve this, we utilize the arm with the standard two-finger gripper. This step is illustrated in Fig. 8. The elevation of the protective film is a direct result of the contact force exerted between the gripper's fingers and the film. It is crucial to accurately calibrate

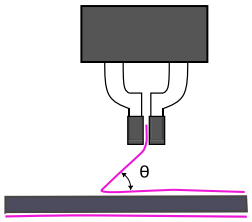

Fig. 10. Step four of the proposed solution: Representation of peeling continuation. The plastic film forms an angle θ with respect to the prepreg.

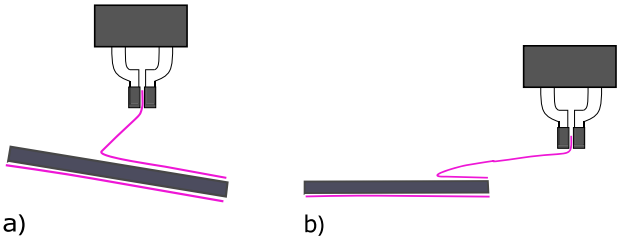

Fig. 11. Consequences of incorrect choices in peeling angle θ and peeling rate $\dot{x}$: (a) represents an excessively high peeling force that lifts the entire ply while (b) represents the excessive space occupation resulting from a too low θ value.

the components of this force. These components are proportional to the gripper's velocity, which follows a vector tangent to the path at the impact points. For simplicity, we employed a linear motion, as illustrated in the upper side of Fig. 8. This motion is defined by two parameters: $h2$ which measures the vertical movement, and L, which measures the horizontal movement.

4.3. Step three: Grasping

Once the protective film's corner is elevated, as depicted on the right side of Fig. 8, it becomes accessible for a grasp using the two-finger gripper. It is noteworthy that the gripper responsible for raising the film's corner is the same one that will grasp it. Consequently, the primary challenge in this phase is navigating the gripper to the optimal grasping position without allowing the film's corner to descend. For this purpose, the gripper rotates around his Z axis and at the same time maintains contact of one of his fingers with the raised corner, as shown in Fig. 9-b. The entire grasping sequence is shown in Fig. 9. Moreover, the starting position of the gripper depends on the prepreg thickness.

4.4. Step four: Peeling continuation

Successful grasping culminates in the film being peeled off (Fig. 10). During this phase, it is imperative to calibrate the optimal peeling angle θ and peeling rate $\dot{x}$. An excessively high peeling Force F runs the risk of lifting the entire ply, a situation depicted in Fig. 11-a. A closer examination of Eq. (5) hints at two potential solutions to mitigate this: a reduction in the peeling rate $\dot{x}$ or a decrease of the angle θ. Lowering the angle, however, necessitates additional workspace, a scenario illustrated in 11-b. Conversely, reducing the velocity implies a prolonged process duration. Therefore, a good selection of these parameters depends on multiple factors: the dimensions of the ply, spatial constraints, and the time allocated for the process.

5. Experimental setup and results

5.1. Experimental setup

The experimental setup is shown in Fig. 1, it makes use of a humanoid robotic structure. This configuration incorporates a primary platform that brings together two UR5e collaborative robots from Universal Robot. As can be seen in the image, the right arm is equipped with an electric vacuum gripper, while the left sports a two-finger gripper. Specifically, the vacuum gripper is a Robotiq EPick model that ensures a vacuum flow at 12L/min at 80% of the vacuum level. Conversely, the two-finger gripper is the Robotiq Hand-E Adaptive model.

To ensure the coordination between the two robotic arms and to carry out custom paths, we exploited the Real-Time Data Exchange (RTDE) interface provided by Universal Robot. This interface operates over the TCP/IP communication protocol. All commands and operations are overseen by a Python script housed in an external computer. This computer establishes a connection with both robot control boxes using an Ethernet cable linked via a switch. Through the RTDE interface, the Python code manages data transmissions, sending and receiving data as the joint positions, speeds, and other parameters associated with the robotic arms. Our protocol included removing the prepreg from the fridge 30 min before the experiments, and each of every 40 trials was done with a new prepreg corner that was not manipulated before. All tests were done with the same environmental conditions, in an environment temperature around 25 °C.

5.2. Results and discussion of the comprehensive framework

To validate the efficiency and reliability of the introduced technique, we conducted a comprehensive set of experiments. The experimental motion sequence is schematically shown in Fig. 12, while the schedule of the motions is provided in the Algorithm 1, and a link to a video-demo experiment can be found in Appendix B.

The inputs of the Algorithm include, on the one hand, the points $P_1 ... P_6$ in solidarity with the ply corner frame selected for the peeling initiation and, on the other hand, the different step-based parameters v_1, v_2, h_1, h_2, L, θ and β.[2]

In Step 3, we adopted a trial-and-error method to determine the best trajectory, focusing on the most frequently occurring position of the raised corner after completing Step 2. We performed 40 tests with different speed profiles for Step 1 and Step 2, while maintaining the same speed for Step 3 and Step 4. Within the algorithm, the function *MoveTCP* controls the End Effector's motion of each robot in Cartesian coordinates, using the Tool Center Point (TCP) as a reference frame. The function *MoveTCP* accepts two arguments, the first one specifies what robot to control, RA (Right Arm) or LA (Left Arm) and the second one specifies the point where to move to. Specifically, $MoveTCP \leftarrow (RA, PX)$ denotes a point-to-point motion of the right arm, from the current position to the target point PX while, $MoveTCP \leftarrow (LA, z)$ indicates the motion of the left arm along the z-axis of the TCP reference frame.

The robot's joints operated under a trapezoidal speed profile. The specifics of the two speed profiles used in the experiments (Speed Profiles A and B) are outlined in Table 1-top, in terms of maximum velocity v_{max} and acceleration a. In each experiment, one of those speed profiles is assigned to Step 1 (v_1), and Step 2 (v_2). Combining these speeds as shown in -bottom results in the three profiles used during the experiments.

The criteria for success in Step 1 involved visually confirming the complete detachment of the film's outer corners. Fig. 14-a represents the successful case, while Fig. 14-b represents the unsuccessful case. In the industrial environment, a visual-based supervision system must be implemented. Success in Step 2 was determined by visually ensuring the corner's elevation at the end of the movement. Fig. 14-c presents the most common unsuccessful case of Step 1. For Step 3, success meant successfully grasping the film. It is important to note that each step's

[2] In our experiments we fixed some of the step parameters: $h_1 \approx 0.2$m, $h_2 \approx 5 \times 10^{-3}$ m, $\beta \approx 0.3$rad, $L \approx 0.05$m and $\theta \approx 0.5$rad.

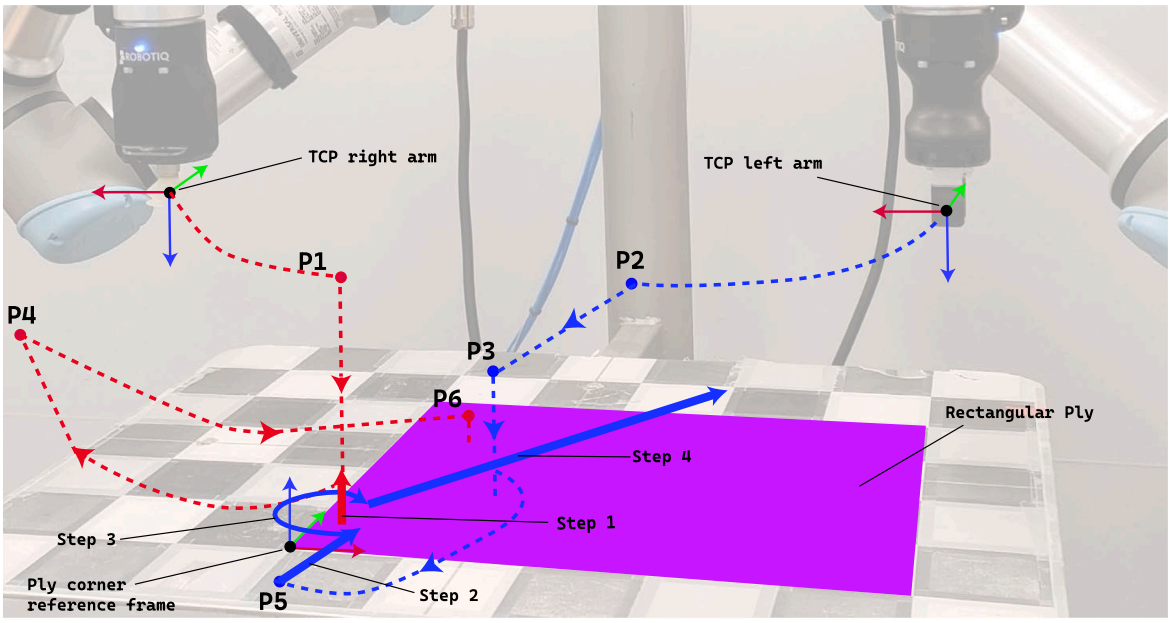

Fig. 12. Illustration of the paths followed by the robotic arms in the experiments. Red paths correspond to the right arm's movements, and the blue ones are for the left arm. Solid lines indicate the primary Steps which we described in Section 4.

Algorithm 1 Dual Robot Motion Scheduling

Inputs:
P1...P6: Robots pre-defined trajectory poses.
v_1, v_2: Step 1 and Step 2 speed profiles.
h_1, h_2: Step 1 and Step 2 heights.
L: Step 2 ply entrance distance.
β: Step 1 angular rotation.
θ: Step 4 peeling angle.

MoveTCP $\leftarrow (RA, P1)$
MoveTCP $\leftarrow (LA, P2)$
MoveTCP $\leftarrow (RA, -z)$
Move until contact with the ply.
MoveTCP $\leftarrow (LA, P3)$
MoveTCP $\leftarrow (LA, -z)$
Move until contact with the ply.
MoveTCP $\leftarrow (RA, -z)$
Move until contact with the ply.
Step 1 $\leftarrow (h_1, \beta)$
MoveTCP $\leftarrow (RA, P4)$
MoveTCP $\leftarrow (RA, P6)$
MoveTCP $\leftarrow (RA, -z)$
Move until contact with the ply.
MoveTCP $\leftarrow (LA, z = 5cm)$
MoveTCP $\leftarrow (LA, P5)$
Step2 $\leftarrow (h_2, L)$
Step3
Step4 $\leftarrow \theta$

success depended on the successful completion of the previous steps. That is, if n is the total number of observations and k_i is the number of successes at Step i, we define the *Success Rate over Previous Step* as

$$\text{SRoPS}_i = \frac{k_i}{k_{i-1}},$$

and the *Success Rate over Total* as

$$\text{SRoT}_i = \frac{k_i}{n}.$$

Table 1
Joint speed profiles parameters for steps 1 and 2.

Joints Speed	v_{max}	a
Speed A	$3.14\frac{rad}{s}$	$38.38\frac{rad}{s^2}$
Speed B	$1.57\frac{rad}{s}$	$19.19\frac{rad}{s^2}$

	Step 1 (Arm 1)	Step 2 (Arm 2)
Profile 1_{AB}	Speed A	Speed B
Profile 2_{BA}	Speed B	Speed A
Profile 3_{AA}	Speed A	Speed A

The experimental results are detailed in Table 2. We can see that the best total success rate of all the steps is 60% and it is achieved with both Steps 1 and 2 at the speed A, which is the highest speed. If we look in more detail, Step 2 worked best when executed at speed A in combination with Step 1 at speed A (93.75%). We can see here the significant influence of motion execution velocity on the completion task in both Step 1 and Step 2. For further analysis, we present in Table 3 the total success rates (SRoT) of all the times Step 1 and Step 2 were executed at speed A and all the times Steps 1 and 2 were executed at speed B. We can see that both steps 1 and 2 work best at the higher speed options.

The final peel-off (Step 4) was tested at different angles θ with a constant velocity (peeling rate) before the tests that we reported here. We confirmed that lowering θ simplifies the peeling but increases the physical space necessary for the task. After different trials, we find out that $\theta \approx 0.5$ rad is a good compromise. Particular attention deserves to think about how to improve the accuracy of the framework we proposed.

- *Step 1:* The execution speed profile significantly influences the process, as evidenced by Eq. (9), which indicates that an increase in angular acceleration α implies a greater detached surface $\mathrm{d}A$, as also supported by our experimental findings. In our experiments, we adopted an electric vacuum generator which has a limited vacuum capacity. An alternative option would involve a vacuum generator based on the Bernoulli effect, which is capable of

Table 2
Success rate of Step 1, Step2, Step 3, and Step 4 at different profiles in terms of Success Rate Over Previous Step (SROPS) and Success Rate Over Total (SROT).

	Profile 1_{BA}		Profile 2_{AB}		Profile 3_{AA}	
	SRoPS	SRoT	SRoPS	SRoT	SRoPS	SRoT
Step 1	50.00%	50.00%	100.00%	100.00%	80.00%	80.00%
Step 2	40.00%	20.00%	40.00%	40.00%	93.75%	75.00%
Step 3	0.00%	0.00%	100.00%	40.00%	80.00%	60.00%
Step 4	0.00%	0.00%	100.00%	40.00%	100.00%	60.00%

The speed profiles are described in . We did 10, 10 and 20 trials for profiles 1, 2 and 3, respectively.

Table 3
SRoT of independently evaluated steps.

	Speed Profile A	Speed Profile B
Step 1	87%	50%
Step 2	81%	40%
Step 3[a]	77%	
Step 4[a]	100%	

[a] The velocity of Step 3 and Step 4 is the same for both speed profiles.

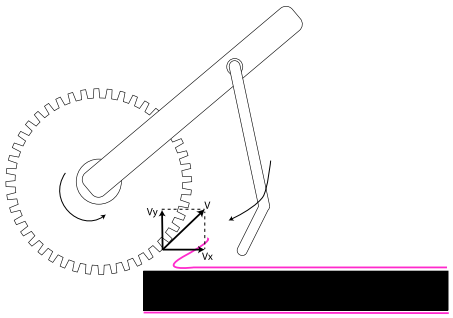

Fig. 13. Gripper composed of a roller and a clamp.

generating greater vacuum power p. This increase in p is expected to enhance the performance (Eq. (12)), in terms of dA. Moreover, Eq. (12) tells us that employing a high-friction material for the vacuum cup is likely to further boost performance. Our current setup has already achieved an accuracy rate of 87% using Speed Profile A, and the use of a Bernoulli-based vacuum generator and high-friction material for the cup might further improve this metric.

- *Step 2:* Also in this case the speed of the execution is critical. This time for a different reason: the velocity of the gripper in the impact points is proportional to the impact force, as we already forecasted in Section 4. Experimentally we have 81% of accuracy for the speed profile A and 40% for speed profile B. Using a linear motion gives little space to play with the horizontal and vertical components of the impact force. This may be the reason why the most common failure case is the one depicted in Fig. 14-c, where the film rolls up instead of raising up. Many works suggest to use of a rotational tool that would be able to increase its vertical component which could bring better results.
- *Step 3:* in this case the main problem is the non-deterministic state of the film corner after the bring-up. A potential solution is a camera-based path planning to optimally navigate the gripper with respect to the film corner state.

A combined roller and clamp gripper, illustrated in Fig. 13 could enhance both Steps 2 and 3. The rotation of the roller can increase the vertical component of the impact speed and this impact speed can be simply regulated by adjusting the roller's rotational speed. Instead of navigating the end effector, as outlined in Step 3, the elevated corner of the material is grasped using the clamp.

5.3. Discussion on the variability of the plies

During the hand layup activity, the laminator handles many kinds of plies, made of different materials and with various shapes. Therefore, a potential robotic system must be capable of managing this variability to be market-relevant. In this section we performed a set of 41 new experiments to evaluate the robustness of the presented system when different materials or shapes are used.

5.3.1. Variability on materials

We performed a set of 21 experiments with different type of prepreg using the most successful velocity profile reported in Table 2. The protective film of this prepreg was found stiffer, exhibiting plastic deformation if pulled too hard. Morover, the adhesive bond between the film and the prepreg appeared to be stronger. To overcome these differences, we implemented a slight modification in our experiment where Step 1 is repeated up to 5 times unless it is detected as successful upon vision inspection. This allowed us to be more versatile if the protective film varies. The first two columns in Table 4 show the overall results. We can see how the success rates are similar to those in the previous experiments, despite the change of material. The only minor drawback encountered is that sometimes we needed to perform step 1 more times. On average, we performed 1.9 suctions for step 1.

According to our experiments, two critical factors in the Step 1 have been identified:

1. *Protective film surface:* A smooth surface is more likely to maintain the vacuum during the execution of Step 1. However, the protective film surface can be rough or present some defects. To overcome this, there are two strategies The first one is to increase airflow in the vacuum cup to compensate for the loss caused by imperfect adherence between the vacuum cup and the surface. The second is to choose a softer surface for the vacuum cup, which can adapt its shape to the protective film.
2. *Stiffness difference between the protective film and the prepreg:* The movement performed in Step 1 deforms the ply. The two layers (protective film and prepreg) experience different deformations, causing the adhesive bonds to break. A significant stiffness difference helps to increase the deformation difference between the two layers, enhancing the performance of Step 1. If the system is dealing with light prepregs, the performance of Step 1 decreases, and the only minor drawback encountered is that it may be necessary to repeat this step several times.

5.3.2. Peeling angle analysis: on the relationship between vacuum cup size and vacuum level

Further experiments were dedicated to investigate the effects of the variability of the lamina shape on the process. These shapes are known a priori; for instance, the plybook serves as a guide for laminators, providing information about the ply shape, fiber orientation, and the specific location where each ply should be positioned. For this reason, the points identified in the PoC (i.e. $P_1, P_2, P_3, \ldots$ on Fig. 12) can be deduced in advance for every ply in the plybook. The critical part of selecting these points is how to choose the peeling angle. We will deal with this problem in this subsection.

Next, we will discuss the need to select the corner in advance, depending on the plyshape, and how to select this corner. We conducted several additional experiments at three different angles, respectively 60°, 90° and 120°, as represented in Fig. 15. The 60° angle performed the worst, with a success rate close to 0%. This happens because the tip of the corner is too far from the vacuum cup, causing it to stick to the prepreg. Therefore, we will not analyze this angle further. Instead, the most interesting results analysis involving the other two angles are reported in Table 4. In the columns 3 and 5 of Table 4 are reported the success rates for the set of 20 experiments with a corner angle of 120°. The results show that the success rate of Step 1 decreases slightly but

Fig. 14. a) Successful Step 1: the corner sides are completely detached b) Unsuccessful Step 1: the corner sides are still attached to the prepreg c) Most common unsuccessful condition of Step 2.

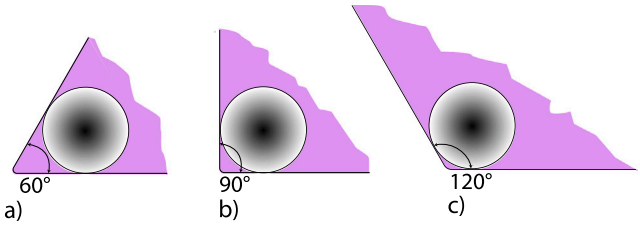

Fig. 15. The figure illustrates Step 1 at various angle widths. The round shape represents the vacuum cup.

Table 4
Results with new material and different corner angles with speed profile 3_{AA}.

	New material 90 degs		New material 120 degs	
	SRoPS	SRoT	SRoPS	SRoT
Step 1	95.24%	95.24%	75.00%	75.00%
Step 2	70.00%	66.67%	66.67%	50.00%

For each new experiment, we repeated 21 and 20 times. Step 1 was applied successively up to 5 times until successful upon vision inspection, and we assumed it was not successful after 5 suctions. In average, for the first experiments, we performed 1.9 suctions, while for the second round, we did 2.67 on average

maintains a good 75% of success rate by performing more repetitions of Step 1, an average of 2.67 suctions at each experiment was obtained. In addition, a decrease in the ability to separate the film can also be observed in Step 2 (see the column SRoPS).

From our results, we can deduce that a general rule of thumb for peeling angle selection is to choose an angle as close to 90° as possible. If there is no angle close to 90°, an angle > 90° should be preferred. To handle angles smaller than 90°, we need to decrease the radius of the vacuum cup, which would place the vacuum cup closer to the tip of the angle. However, according to Eq. (12), we need to increase the vacuum pressure to maintain the same performance.

To conclude this section, depending on the shapes reported in the plybook, we must find the right compromise between the vacuum level and the radius of the vacuum cup. For "difficult" corners, it may be necessary to reduce the size of the vacuum cup and increase the vacuum level.

6. Conclusions

A complete framework for protective film removal using two collaborative robots has been developed and tested, introducing an innovative method to initiate the process. This research integrates preliminary observations with the experimental findings to establish an optimal approach to this challenge in an industrial setting, potentially leading to the development of new market-ready devices. To the best of the author's knowledge, this is the first study that provides a comprehensive solution with experimental validation for this problem, the first time posed in 1996 [16]. Previous works [17–19] provided only partial solutions or lacked experimental evidence and observations. In 2017 [5] this issue was considered an open problem.

This work represents the first step towards the integration of a robotic system for automatic film removal into manual layup tasks. From an economic point of view, this integration would be facilitated if the use of the robotic system was planned for a wider range of tasks, such as the co-transport of layers, already mentioned earlier in this paper. Engineering efforts should therefore focus on providing the robotic system with greater autonomy (which is one of the main challenges of current research) in order to make it capable of handling more tasks with the same hardware.

Further research efforts would be to address the integration of collaborative robots in industrial environments with human presence and proximity, and in rescheduling the tasks of normal hand layup activity.

In conclusion, we believe that addressing this problem is significant as it eliminates a tedious and valueless task from manual processes and would make more efficient automated or semi-automated systems.

CRediT authorship contribution statement

Renat Kermenov: Conceptualization, Data curation, Investigation, Methodology, Software, Validation, Writing – original draft. **Sergi Foix:** Investigation, Supervision, Writing – review & editing. **Júlia Borràs:** Data curation, Investigation, Supervision, Writing – review & editing. **Vincenzo Castorani:** Investigation, Resources, Supervision, Writing – review & editing. **Sauro Longhi:** Investigation, Resources, Supervision. **Andrea Bonci:** Funding acquisition, Methodology, Conceptualization, Project administration, Resources, Supervision, Writing – review & editing.

Declaration of competing interest

The authors declare that they have no known competing financial interests or personal relationships that could have appeared to influence the work reported in this paper.

Acknowledgments

This research was partially funded by European project Horizon Europe "EDIH4Marche" (European Digital Innovation Hub for Marche), Call DIGITAL-2021-EDIH-01, Grant Agreement no. 101084027 on topic DIGITAL-2021-EDIH-INITIAL-01 (DIGITAL Simple Grants Acton) and project CHLOE-GRAPH (PID2020-118649RB-I00) funded by Ministerio de Ciencia, Innovación y Universidades/Spanish State Research Agency (AEI) /10.13039/501100011033.

Appendix A. Definitions

1. *Layup* (or *Lamination*) refers to a process that merges two or more layers of a material, to create a new composite with improved properties (mechanical, electrical, chemical, etc.). In this article, we considered the layup of fibrous materials, such as carbon fiber. Moreover, we consider the manual process, predominantly used for the automotive and aerospace market, known as *hand layup/lamination*. For high-performance components, the layers in this process are made of *prepregs*.

2. *Prepreg* is a unidirectional or woven fabric pre impregnated with a specific resin. In composite manufacturing, prepreg rolls are cut into various shapes to form different layers of the composite component. These cut prepreg pieces are usually called *plies* or *laminas*.
3. *Curing Process* involves applying heat and pressure to the laminated component, causing the resin in the prepreg to transition from a liquid to a solid state. It is an essential process for achieving the desired mechanical properties of the final component.

Appendix B. Supplementary data

Supplementary material related to this article can be found online at https://doi.org/10.1016/j.rcim.2024.102899.

Data availability

No data was used for the research described in the article.

References

[1] D.H.-J. Lukaszewicz, C. Ward, K.D. Potter, The engineering aspects of automated prepreg layup: History, present and future, Composites B 43 (3) (2012) 997–1009, http://dx.doi.org/10.1016/j.compositesb.2011.12.003.

[2] M. Elkington, D. Bloom, C. Ward, A. Chatzimichali, K. Potter, Hand layup: understanding the manual process, Adv. Manuf.: Polymer Compos. Sci. 1 (3) (2015) 138–151, http://dx.doi.org/10.1080/20550340.2015.1114801.

[3] J. de Kruijk, Automated Composite Manufacturing Using Robotics Lowers Cost, Lead-Time and Scrap Rate, Netherlands Aerospace Centre NLR, 2018.

[4] F.C. Campbell Jr., Manufacturing Processes for Advanced Composites, Elsevier, 2003.

[5] M. Elkington, A. Sarkytbayev, C. Ward, Automated composite draping: A review, in: International SAMPE Technical Conference, 2017, pp. 1672–1686.

[6] R.K. Malhan, A.V. Shembekar, A.M. Kabir, P.M. Bhatt, B. Shah, S. Zanio, S. Nutt, S.K. Gupta, Automated planning for robotic layup of composite prepreg, Robot. Comput.-Integr. Manuf. 67 (2021) http://dx.doi.org/10.1016/j.rcim.2020.102020.

[7] R.K. Malhan, A.V. Shembekar, R.J. Joseph, A.M. Kabir, P.M. Bhatt, B. Shah, W. Zhao, S. Nutt, S.K. Gupta, Asmart robotic cell for automating composite prepreg layup, in: International SAMPE Technical Conference, 2020-June, 2020.

[8] D. De Schepper, G. Schouterden, K. Kellens, E. Demeester, Human-robot mobile co-manipulation of flexible objects by fusing wrench and skeleton tracking data, Int. J. Comput. Integr. Manuf. 36 (1) (2023) 30–50, http://dx.doi.org/10.1080/0951192X.2022.2081362.

[9] G. Nicola, S. Mutti, E. Villagrossi, N. Pedrocchi, Depth image-based deformation estimation of deformable objects for collaborative mobile transportation, in: 2023 32nd IEEE International Conference on Robot and Human Interactive Communication (RO-MAN), IEEE, 2023, pp. 2658–2664.

[10] G. Nicola, E. Villagrossi, N. Pedrocchi, Co-manipulation of soft-materials estimating deformation from depth images, Robot. Comput.-Integr. Manuf. 85 (2024) http://dx.doi.org/10.1016/j.rcim.2023.102630.

[11] S. Makris, E. Kampourakis, D. Andronas, On deformable object handling: Model-based motion planning for human-robot co-manipulation, CIRP Ann 71 (1) (2022) 29–32, http://dx.doi.org/10.1016/j.cirp.2022.04.048.

[12] D. Andronas, E. Kampourakis, K. Bakopoulou, C. Gkournelos, P. Angelakis, S. Makris, Model-based robot control for human-robot flexible material co-manipulation, in: IEEE International Conference on Emerging Technologies and Factory Automation, ETFA, 2021-September, 2021, http://dx.doi.org/10.1109/ETFA45728.2021.9613235.

[13] G. Papadopoulos, D. Andronas, E. Kampourakis, N. Theodoropoulos, P.S. Kotsaris, S. Makris, On deformable object handling: multi-tool end-effector for robotized manipulation and layup of fabrics and composites, Int. J. Adv. Manuf. Technol. 128 (3–4) (2023) 1675–1687, http://dx.doi.org/10.1007/s00170-023-11914-z.

[14] Y.-W. Chen, R.J. Joseph, A. Kanyuck, S. Khan, R.K. Malhan, O.M. Manyar, Z. McNulty, B. Wang, J. Barbic, A digital twin for automated layup of prepreg composite sheets, Trans. ASME, J. Manuf. Sci. Eng. 144 (4) (2022) http://dx.doi.org/10.1115/1.4052132.

[15] Y. Zhang, L. Yuan, W. Liang, X. Xia, Z. Pang, 3D-SWiM: 3D vision based seam width measurement for industrial composite fiber layup in-situ inspection, Robot. Comput.-Integr. Manuf. 82 (2023) http://dx.doi.org/10.1016/j.rcim.2023.102546.

[16] R. Buckingham, G. Newell, Automating the manufacture of composite broadgoods, Composites A 27 (3 PART A) (1996) 191–200, http://dx.doi.org/10.1016/1359-835X(96)80001-9.

[17] A. Björnsson, J.-E. Lindback, K. Johansen, Automated removal of prepreg backing paper - A sticky problem, SAE Technical Papers 7 (2013) http://dx.doi.org/10.4271/2013-01-2289.

[18] C. Ward, V. Bhatnagar, K. Potter, Developing an automated system for the removal of protective films from pre-preg material, to remove a manufacturing bottleneck in terms of pick and place automation, SAMPE SETEC 13 (2013) 11–12.

[19] D. Kupzik, F. Ballier, J. Lang, S. Coutandin, J. Fleischer, Development and evaluation of concepts for the removal of backing foils from prepreg for the automated production of UD reinforced SMC parts, in: ECCM 2018 - 18th European Conference on Composite Materials, 2020.

[20] V. Basile, G. Fontana, F. Modica, M. Valori, L. Rebaioli, S. Ruggeri, S.P. Negri, I. Fassi, Numerical and experimental study on protective film removal towards the automation of flexible electronics assembly, Int. J. Adv. Manuf. Technol. 122 (11–12) (2022) 4375–4387, http://dx.doi.org/10.1007/s00170-022-09884-9.

[21] M. Valori, V. Basile, S. Ruggeri, G. Fontana, S.P. Negri, J.A. Mulet Alberola, I. Fassi, Assembly of film coverlays: Development of a configurable gripper for process automation, Procedia Manuf. 55 (C) (2021) 80–87, http://dx.doi.org/10.1016/j.promfg.2021.10.012.

[22] H. Jones, A. Chatzimichali, R. Middleton, K. Potter, C. Ward, Exploring the discrete tools used by laminators in composites manufacturing: application of novel concept, Adv. Manuf.: Polym. Compos. Sci. 1 (4) (2015) 185–198, http://dx.doi.org/10.1080/20550340.2015.1105613.

[23] A. Endruweit, G.Y. Choong, S. Ghose, B.A. Johnson, D.R. Younkin, N.A. Warrior, D.S. De Focatiis, Characterisation of tack for uni-directional prepreg tape employing a continuous application-and-peel test method, Composites A 114 (2018) 295–306, http://dx.doi.org/10.1016/j.compositesa.2018.08.027.

[24] A. Gent, A. Kinloch, Adhesion of viscoelastic materials to rigid substrates. III. Energy criterion for failure, J. Polym. Sci. A-2: Polym. Phys. 9 (4) (1971) 659–668, http://dx.doi.org/10.1002/pol.1971.160090408.

[25] K. Kendall, Thin-film peeling-the elastic term, J. Phys. D: Appl. Phys. 8 (13) (1975) 1449–1452, http://dx.doi.org/10.1088/0022-3727/8/13/005.

[26] A. Björnsson, M. Jonsson, K. Johansen, Automated material handling in composite manufacturing using pick-and-place systems – a review, Robot. Comput.-Integr. Manuf. 51 (2018) 222–229, http://dx.doi.org/10.1016/j.rcim.2017.12.003.

[27] G. Mantriota, A. Messina, Theoretical and experimental study of the performance of flat suction cups in the presence of tangential loads, Mech. Mach. Theory 46 (5) (2011) 607–617, http://dx.doi.org/10.1016/j.mechmachtheory.2011.01.003.